PAPER

Reinventing a p-type doping process for stable ZnO light emitting devices

IOP Publishing Journal of Physics D: Applied Physics
J. Phys. D: Appl. Phys. **51** (2018) 225104 (4pp) https://doi.org/10.1088/1361-6463/aabe49

Reinventing a p-type doping process for stable ZnO light emitting devices

Xiuhua Xie, Binghui Li, Zhenzhong Zhang and Dezhen Shen

State Key Laboratory of Luminescence and Applications, Changchun Institute of Optics, Fine Mechanics and Physics, Chinese Academy of Sciences, Changchun 130033, People's Republic of China

E-mail: binghuili@163.com and shendz@ciomp.ac.cn

Received 24 February 2018, revised 7 April 2018
Accepted for publication 16 April 2018
Published 8 May 2018

Abstract

A tough challenge for zinc oxide (ZnO) as the ultraviolet optoelectronics materials is realizing the stable and reliable p-type conductivity. Self-compensation, coming from native donor-type point defects, is a big obstacle. In this work, we introduce a dynamic N doping process with molecular beam epitaxy, which is accomplished by a Zn, N-shutter periodic switch (a certain time shift between them for independent optimization of surface conditions). During the epitaxy, N adatoms are incorporated under the condition of (2×2) + Zn vacancies reconstruction on a Zn-polar surface, at which oxygen vacancies (V_O), the dominating compensating donors, are suppressed. With the p-ZnO with sufficient holes surviving, N concentration ~1×10^{19} cm^{-3}, is employed in a p-i-n light emitting devices. Significant ultraviolet emission of electroluminescence spectra without broad green band (related to V_O) at room-temperature are demonstrated. The devices work incessantly without intentional cooling for over 300 h at a luminous intensity reduction of one order of magnitude under the driving of a 10 mA continuous current, which are the demonstration for p-ZnO stability and reliability.

Keywords: zinc oxide, p-type, self-compensation, doping

(Some figures may appear in colour only in the online journal)

1. Introduction

Zinc oxide (ZnO), due to its excellent optoelectronic properties, has extensive applications in many fields [1–4]. Especially as one of the most promising ultraviolet low threshold lasing candidates has been extensively studied on p-type doping [5–8], which is one of the most challenging issues. Previously, among p-type dopants, the nitrogen (N) has been proven as a very suitable acceptor [9–12]. Although a few of the significant results have been achieved in the aspects of p-n homojunction electroluminescence (EL) based on N doping [11–14], the stability and reliability of such devices have not yet reached expectations, which is attributed to the low doping efficiency. Currently, two main negative facts are generally invoked as responsible for low efficiency of p-type doping: low-incorporation and self-compensation [15, 16]. The low-incorporation is mainly due to the smaller bound energy of Zn–N compared to Zn–O [17, 18]. At present, there are many technical means to increase the amount of N incorporated from the perspectives of quantity and energy of N bonding, such as low-temperature epitaxy, polarity control, and isoelectronic impurity assisted [8, 19, 20]. On the other hand, however, the self-compensation occurs during epitaxial growth, which means the acceptors are compensated by native point defects, resulting in not enough free holes to survive [16]. Unfortunately, there is still no effective way to suppress self-compensation. In order to solve this problem, we need to re-focus on the process of epitaxial growth, which is the key to the formation of impurities and defects. Specifically, during the growth, epitaxial films are usually divided into surface and interior parts [21]. The adatoms are always coated first to the surface and become the interior of the film. At a given substrate temperature, the inside of the film is equivalent to being annealed and its atoms are in a thermodynamic equilibrium. At the same time, the atoms on the surface undergo complex thermodynamic non-equilibrium processes with each other,

which is also the part from which self-compensation takes place. Therefore, the control of self-compensation can be realized by adjusting the external surface process.

As we know, during certain polar epitaxial growth, specific native point defects can be formed on the surface layer, which comes from the offset to the spontaneous polarization breaking on the polar surface [22–25]. Under extreme oxygen-rich conditions, Zn vacancies (V_{Zn}), acceptor-type defects for ZnO, tend to form on Zn-polar (0 0 0 2) surface, while oxygen vacancies (V_O), donor-type defects, are suppressed [25, 26]. Based on this, combined the processes of N doping and V_{Zn} formation on Zn-polar surface, the compensation from V_O will be inhibited, as well as the introduction of V_{Zn} assistance, which is very beneficial for improving the efficiency of the p-type doping.

We have recently reported on manipulation of V_{Zn} in ZnO via Zn-polar surface (2 × 2) reconstruction, during shutter non-synchronous controlled molecular beam epitaxy (MBE) growth, where V_O have been suppressed [26]. This method is practicable for further p-type doping process. In this work, based on the previous results, we introduced a dynamic nitrogen-doped epitaxial growth scheme on Zn-polar surface, which achieve the N incorporation with self-compensation inhibition. Then, p-n homojunction light emitting devices have been obtained successfully. Element profiles of homojunction were obtained by secondary ion mass spectrometry (SIMS). EL spectra of different drive currents were also obtained at room-temperature. Subsequently, the luminous life of devices has been tested.

2. Experimental details

Samples were grown in MBE system (DCA-P600) equipped with oxford radio-frequency (RF) atom sources (HD25) with ion removal control for active O and N, and solid-source effusion cells for Zn and Mg. In order to enhance the proportion of radiation in the intrinsic zone, an electron blocking layer, N-doped MgZnO, was inserted between the p-type and the intrinsic layer. The beam equivalent pressure ratio (BPR) of [Mg]/[Zn] is about 1/100. The N_2 flow rate is about 2.5 sccm with a RF power of 350 W. Other details of epitaxial growth conditions can be seen from our previous work, including uniform Zn-polar growth, high quality intrinsic and low resistivity ZnO epitaxy [26–29]. Here it is necessary to be specific about the doping process of N. As can been seen from figure 1, a schematic diagram of a dynamic N doping scheme, the N-shutter periodic switch has a certain degree of phase shift relative to the Zn-shutter. When (2 × 2) + V_{Zn} surface reconstruction is achieved, logically, the Zn-shutter 'ON' corresponds to a virtual V_{Zn} source shutter 'OFF', and vice versa, red line in figure 1. In order to ensure that Zn and N atoms have sufficient time to adsorb the entire surface while allowing sufficient surface energy relaxation time to ensure (2 × 2) surface reconstruction, 1–2 monolayers have been grown per cycle. The ON/OFF time of shutters is determined using reflection high-energy electron diffraction (RHEED) intensity variations. Each peak of RHEED intensity represents

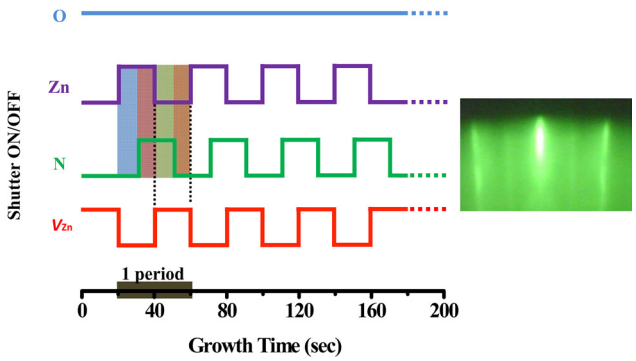

Figure 1. Schematic drawing of Zn-, N-shutter switch action during the dynamic N doping. Under (2 × 2) surface reconstruction condition, the Zn-shutter 'OFF' corresponds to a virtual V_{Zn} source shutter 'ON'. Inset: RHEED pattern shows the (2 × 2) reconstructed ZnO surface during the whole N doping process.

the forming of a new monolayer [30]. In this work, turn-on/off time of shutters all uses 20 s, while the N-shutter has a 10 s delay relative to Zn-shutter. In detail, a set of Zn, N, V_{Zn} shutter linkage is divided into four stages. Firstly, Zn beam atoms have been taken the lead in arriving at the film surface, where the ratio of O/Zn is slightly larger to ensure 2D growth under the Zn-polar [31]. N beam atoms arriving in sequence. N bonds with Zn occupy O sites (N_O). Fermi level tends to the valence band, and then the energy to form the donor V_O is reduced. Taking into account the fact that the formation of V_O needs a certain relaxation time, at this point, the Zn-shutter closed to create an extreme oxygen-rich environment. Therefore, the V_O has been suppressed, while due to the continuous arrival of N atoms, the probability of desorption of surface N atoms is reduced. Finally, the N-shutter has also been closed, to avoid the polarity inversion caused by excess N atoms (similar to Mg doping GaN) [32, 33]. The streaky (2 × 2) RHEED pattern (figure 1 inset), an indication of Zn-polar surface and V_{Zn} formation, stays stable during the whole N doping process, which further proves that V_O are suppressed in the second and third stages.

3. Results and discussion

A p-i-n (p-ZnO/N:MgZnO/i-ZnO/n-ZnO) structure was grown for next-step device fabrication (figure 2 inset). In order to accurately and intuitively give the depth distribution of N, Mg in the sample, dopants profiles were measured by SIMS, using cesium 133 ($^{133}Cs^+$) and O_2^+ as the primary ion beam (CAMECA IMS-7F). The elements (N, Mg) have been calibrated by standard sample. As illustrated in figure 2, the N:$Mg_{0.05}Zn_{0.95}O$ layer is about 100 nm, which serves to block the electrons injected from the n-side and increasing the emission ratio of the i-layer. There is a MgZnO sheet (Mg concentration ~2 × 10^{19} cm^{-3}), which may come from phase separation of MgZnO induced by atoms beam instability at the moment of the shutter just opening. The p-ZnO layer is about 450 nm with N concentration ~1 × 10^{19} cm^{-3}. The conductivity of N doped ZnO films (single-layer films grown under the same N doping conditions for Hall testing)

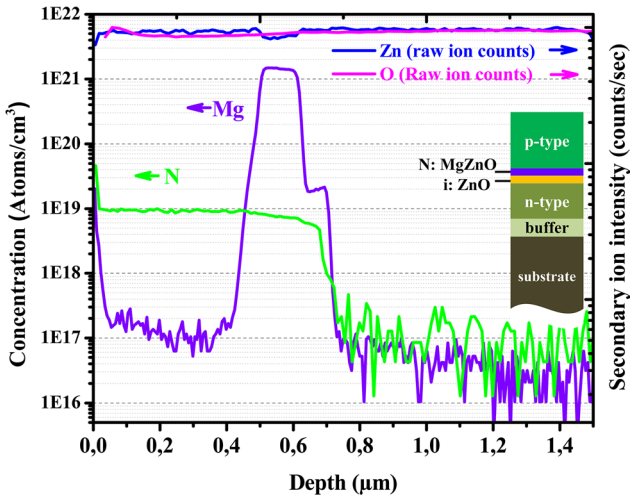

Figure 2. Profiles of Mg, N as a function of depth into the substrate from the surface. The N concentration is ~1 × 10^{19} cm^{-3} in p-type ZnO layer. The $Mg_{0.05}Zn_{0.95}O$ electron blocking is about 100 nm. The inset shows the depict cross-sectional schematics for the p-i-n (p-ZnO/N:MgZnO/i-ZnO/n-ZnO) structure.

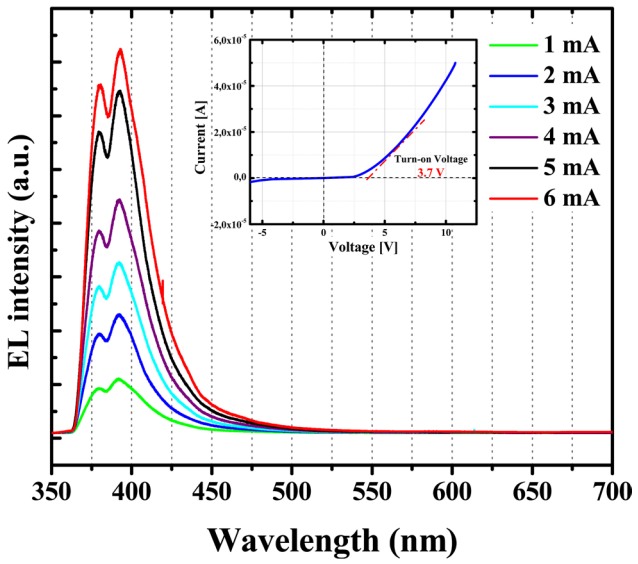

Figure 3. EL spectra under different driving currents at room-temperature. There are no V_O-related green bands, around 550 nm. The inset shows the rectifying current–voltage characteristics of the p-i-n device with a turn-on voltage of about 3.7 V.

has been measured by Hall with van der Pauw configuration at room temperature. N doped ZnO films exhibit p-type conductivity, with a hole concentration of about 5 × 10^{16} cm^{-3} and a mobility of about 3 cm^2 V^{-1} s^{-1}. The total N undoped layer is ~800 nm, including i-ZnO (~50 nm), n-ZnO (~400 nm) and buffer layer (~350 nm), which is determined by atoms beam conditions. The n-type ZnO is achieved by slightly deviating the Zn/O stoichiometry of the epitaxial process [28].

The preparation of the light emitting devices using a standard photolithography process. Hydrochloric acid solution (1.5 mol l^{-1}, 25 °C) was used to etch the upper portion of the film to reach the n-type ZnO layer. The n-side electrode is Ti/Au, which is obtained by sputtering. While the p-side electrode is Ni/Au that was prepared by thermal evaporation. The device exhibits significant rectification characteristics with a turn-on voltage of 3.7 V, as can be seen from the inset of figure 3. There are two significant EL peaks at room-temperature, located at 380 nm and 392 nm, which come from the luminescence of MgZnO and i-ZnO layer, respectively. The luminescence of the p-ZnO layer in the longer wavelength band has not been observed [11, 13], indicating that the MgZnO electron blocking layer was already functioning. Both peaks showed an insignificant redshift with the increase of driving current. Therefore, the heating effect is very weak, which indicates that electrodes (p and n sides) have a very small contact resistance and a higher crystalline quality of the active layer. Especially, the broad green emission band (often observed in ZnO-based light emitting devices [11, 13, 20], around 550 nm, related to V_O) has not been observed.

The luminous lifetime of a single device has been tested, which is a criterion for stability. The device worked at room-temperature without intentional cooling system. The constant drive current is 10 mA and keeps working, incessantly, during the whole lifetime measurement. As illustrated in the figure 4, more than 300 h of continuous work, the luminous intensity of the device was down by one order of magnitude, compared to

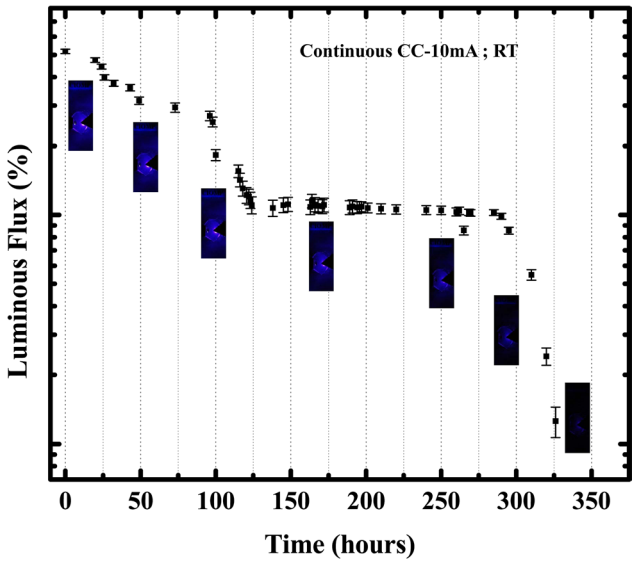

Figure 4. Luminous intensity of the device versus time with the constant drive current of 10 mA at room-temperature. Insets: optical microscope images of the device taken at different stages.

the initial intensity. Lifetime test ends when luminous intensity decays to 1/50 the first. Our results have been greatly improved compared with previous reports [20, 34, 35]. Actually, this degraded device can still be lit after six months later, although the luminous intensity is weak. The EL and lifetime results of our ZnO-based homojunctions confirmed that the p-type ZnO obtained by a dynamic nitrogen-doped process is reliable and stable.

4. Conclusions

In a summary, we have introduced the dynamic N doping process of ZnO films, which can suppress the self-compensation,

effectively. The ZnO-based p-i-n homojunctions have been realized, successfully. EL spectra exhibited significant ultraviolet emissions without broad green band at room temperature under different driving current. Our devices have been operating continuously for over 300 h at a luminous intensity reduction of one order of magnitude. Precise control of the film surface conditions during doping provides a practicable approach for effective p-type doping. Device performance improvement in the future can be achieved via N concentration further increasing and, in particular, device technique optimization.

Acknowledgments

The authors gratefully acknowledge support from the National Natural Science Foundation of China (NSFC) under Grant Nos. 61505200 and 11727902.

ORCID iDs

Binghui Li https://orcid.org/0000-0002-2210-7031

References

[1] Lai Y Y, Lan Y P and Lu T C 2013 *Light Sci. Appl.* **2** e76
[2] Shrestha P K, Chun Y T and Chu D 2015 *Light Sci. Appl.* **4** e259
[3] Zang Z, Zeng X, Du J, Wang M and Tang X 2016 *Opt. Lett.* **41** 3463
[4] Li C, Zang Z, Han C, Hu Z, Tang X, Du J, Leng Y and Sun K 2017 *Nano Energy* **40** 195
[5] Tang Z K, Wong G K L, Yu P, Kawasaki M, Ohtomo A, Koinuma H and Segawa Y 1998 *Appl. Phys. Lett.* **72** 3270
[6] Bagnall D M, Chen Y F, Zhu Z, Yao T, Koyama S, Shen M Y and Goto T 1997 *Appl. Phys. Lett.* **70** 2230
[7] Look D C 2001 *Mater. Sci. Eng.* B **80** 383
[8] Özgür Ü, Alivov Ya I, Liu C, Teke A, Reshchikov M A, Doğan S, Avrutin V, Cho S-J and Morkoçd H 2005 *J. Appl. Phys.* **98** 041301
[9] Look D C, Reynolds D C, Litton C W, Jones R L, Eason D B and Cantwell G 2002 *Appl. Phys. Lett.* **81** 1830
[10] Tsukazaki A, Kubota M, Ohtomo A, Onuma T, Ohtani K, Ohno H, Chichibu S F and Kawasaki M 2005 *Japan. J. Appl. Phys.* 2 **44** L643
[11] Jiao S J, Zhang Z Z, Lu Y M, Shen D Z, Yao B, Zhang J Y, Li B H, Zhao D X, Fan X W and Tang Z K 2006 *Appl. Phys. Lett.* **88** 031911
[12] Tsukazaki A *et al* 2005 *Nat. Mater.* **4** 42
[13] Wei Z P, Lu Y M, Shen D Z, Zhang Z Z, Yao B, Li B H, Zhang J Y, Zhao D X, Fan X W and Tang Z K 2007 *Appl. Phys. Lett.* **90** 042113
[14] Nakahara K *et al* 2010 *Appl. Phys. Lett.* **97** 013501
[15] Pearton S J and Ren F 2014 *Int. Mater. Rev.* **59** 61
[16] Walsh A and Zunger A 2017 *Nat. Mater.* **16** 964
[17] Chen M M *et al* 2015 *J. Alloys Compd.* **622** 719
[18] Hirai M and Kumar A 2007 *J. Vac. Sci. Technol.* A **25** 1534
[19] Lautenschlaeger S *et al* 2012 *Phys. Rev.* B **85** 235204
[20] Chen A Q, Zhu H, Wu Y Y, Chen M M, Zhu Y, Gui X C and Tang T K 2016 *Adv. Funct. Mater.* **26** 3696
[21] Ayers J E 2007 *Heteroepitaxy of Semiconductors: Theory, Growth, and Characterization* (Boca Raton, FL: CRC Press)
[22] Kresse G, Dulub O and Diebold U 2003 *Phys. Rev.* B **68** 245409
[23] Valtiner M, Todorova M, Grundmeier G and Neugebauer J 2009 *Phys. Rev. Lett.* **103** 065502
[24] Lai J H, Su S H, Chen H-H, Huang J C A and Wu C-L 2010 *Phys. Rev.* B **82** 155406
[25] Pal S, Jasper-Tönnies T, Hack M and Pehlke E 2013 *Phys. Rev.* B **87** 085445
[26] Xie X H, Li B H, Zhang Z Z and Shen D Z 2017 *J. Phys. D: Appl. Phys.* **50** 325304
[27] Liu J S, Shan C X, Wang S P, Sun F, Yao B and Shen D Z 2010 *J. Cryst. Growth* **312** 2861
[28] Liu J S, Shan C X, Wang S P, Li B H, Zhang Z Z and Shen D Z 2012 *J. Cryst. Growth* **347** 95
[29] Xie X H, Li B H, Zhang Z Z and Shen D Z 2018 *AIP Adv.* **8** 035115
[30] Sadofev S, Blumstengel S, Cui J, Puls J, Rogaschewski S, Schäfer P, Sadofyev Yu G and Henneberger F 2005 *Appl. Phys. Lett.* **87** 091903
[31] Kato H, Sano M, Miyamoto K and Yao T 2004 *J. Cryst. Growth* **265** 375
[32] Pezzagna S, Venneguès P, Grandjean N and Massies J 2004 *J. Cryst. Growth* **269** 249
[33] Ramachandran V, Feenstra R M, Sarney W L, Salamanca-Riba L, Northrup J E, Romano L T and Greve D W 1999 *Appl. Phys. Lett.* **75** 808
[34] Liu J S, Shan C X, Shen H, Li B H, Zhang Z Z, Liu L, Zhang L G and Shen D Z 2012 *Appl. Phys. Lett.* **101** 011106
[35] Shan C X, Liu J S, Lu Y J, Li B H, Ling F C and Shen D Z 2015 *Opt. Lett.* **40** 3041